Eur. Phys. J. D **25**, 77–87 (2003)
DOI: 10.1140/epjd/e2003-00080-2

THE EUROPEAN PHYSICAL JOURNAL D

Near dipole-dipole effects in a V-type medium with vacuum induced coherence

O.G. Calderón[a], M.A. Antón[b], and F. Carreño[c]

Escuela Universitaria de Óptica, Universidad Complutense de Madrid, C/ Arcos de Jalón s/n, 28037 Madrid, Spain

Received 2 August 2002 / Received in final form 17 January 2003
Published online 24 April 2003 –

Abstract. In this paper we investigate the influence of the local field correction (LFC) on the optical behavior of a closed V-type system. We consider a V configuration such that quantum interference between the two decay channels to the ground atomic level is important. When the two optical transitions are coupled by one laser field we find that LFC does not destroy the non-absorption resonance that usually appears due to quantum interference. On the other hand, the absorption profile is deformed due to the presence of LFC. We have also studied the case of a driving laser field coupling one of the optical transitions, and a probe laser field coupling the other one. In this field configuration the local field modifies substantially the optical response. We have found that the system can switch between absorption and gain by controlling the near dipole-dipole parameter. On the other hand, the relative phase between the pump and probe fields allow us to change the system from absorption to gain.

PACS. 42.50.Gy Effects of atomic coherence on propagation, absorption, and amplification of light; electromagnetically induced transparency and absorption – 42.50.Ct Quantum description of interaction of light and matter; related experiments – 42.50.Fx Cooperative phenomena in quantum optical systems

1 Introduction

In recent years, there has been considerable interest in quantum interference and coherence effects in multilevel atom systems induced by coherent electromagnetic fields. Many phenomena, such as electromagnetically induced transparency (EIT) [1,2], lasing without inversion (LWI) [3–5], refractive index enhancement without absorption [6–8], and giant nonlinearity [9–11], have been predicted and experimentally demonstrated and have modified the way we look at photon absorption and emission processes. During the last decade, many different schemes have been studied in Λ and V atoms where the coherence is created by the driving fields.

Another way of generating coherence is connected with the relaxation processes such as spontaneous emission. It is well-known how quantum coherence can be created in interactions involving a common bath with a set of closely lying states. This rather contraintuitive phenomenon has been shown by Agarwal [12]. If the two upper levels are very close and damped by the usual vacuum interactions, spontaneous emission cancellation can take place [13–16]. Then, the two decay pathways from the excited doublet to the ground state are not independent, which offers the possibility to trap population in the excited levels when some particular conditions hold [5,17–20]. Quantum interference between the two transition channels connecting the ground-level is responsible for many novel effects, such as dark spectral lines [21,22], narrow resonances and probe transparency [16], lasing without population inversion [1,3], phase dependent line shapes [19,20], etc. Although the existence of the interference effects depends on a very stringent condition, *viz.*, the dipole matrix moments for the two closely lying states decaying to a common final state should be nonorthogonal [12], several new methods to bypass this strict condition have been proposed [23]. Furthermore, Agarwal and Patnaik have recently shown that the anisotropy of the vacuum of the electromagnetic field could lead to quantum interference among the decay channels of closely lying states, even if the dipole matrix elements were orthogonal [24].

All previous studies in the emission cancellation in V-type atoms with closely excited levels have been carried out in the framework of three-level Maxwell-Bloch equations in dilute media, that is, the interactions between atoms, which are manifested through dipole-dipole interactions, have been ignored. This procedure is generally accurate for large interatomic separations and low values of dipole moments. However, when the atomic system is

[a] e-mail: oscargc@opt.ucm.es
[b] e-mail: antonm@fis.ucm.es
[c] e-mail: ferpo@fis.ucm.es

working near resonance, the atoms can acquire a large dipole moment. Moreover, if the relative distance between atoms in some dense-atom system is not large, the local field correction (LFC) or near dipole-dipole (NDD) interaction between atoms cannot be neglected. In this case, the effective field acting on an atom is the local field, which is due to both the external field and the remaining atomic dipoles of the sample [25]. The inclusion of LFC in Maxwell-Bloch equations has been extensively considered for two-level atoms. As a result, Bloch equations become nonlinear regarding the population inversion and polarization amplitude, which leads to many interesting phenomena, such as self-phase modulation in self-induced transparency [26,27], linear and nonlinear spectral shifts [28,29], novel inversion and ultrafast switching effects [30], and intrinsic optical bistability (IOB) [31–34]. This last phenomenon has been experimentally confirmed by Hehlen *et al.* by using Yb^{3+} ions in a $Cs_3Y_2Br_9$ crystal [35,36]. The local-field renormalization of the spontaneous emission rate of a two level atom embedded in an absorptive and dispersive linear dielectric has been obtained from a fully microscopic quantum-electrodynamic derivation by several authors [37–47].

Obviously, the coherence and interference effects in multilevel atoms are not immune to the influence of local field. In fact, an enhancement of the inversionless gain by more than two orders of magnitude have been obtained by Dowling and Bowden in lasing without inversion by using a coherently prepared three-level Λ system [48]. A piezophotonic switching effect has been found by Manka *et al.* in the same atomic system [49] when the density of the medium slightly changes. The characteristics of coherent trapping states in a dense medium composed of Λ atoms have been investigated by Jyotsna and Agarwal [50].

The aim of this paper is to investigate the influence of near dipole-dipole interaction on the steady-state population inversion and atomic polarization of a closed V-type atom when quantum interference between the two decay channels to the ground atomic level is considered. Our atomic system is similar to that studied by Paspalakis and Knight [20] but the effect of the local field is included. Specifically, we consider two different field configurations: a single laser field coupling simultaneously the ground state with the two closely excited levels, and a degenerate pump-probe configuration. In the last case, the interplay between the local field and the relative phase between both fields gives an enhancement of the gain and changes the system from absorption to gain when the relative phase between the pump and probe fields is varied.

The paper is organized as follows: Section 2 establishes the model, *i.e.*, the Hamiltonian of the system and the evolution equation of the atomic operators by assuming the rotating wave approximation. The effects of the local field in absorption and population inversion when the atom interacts with an external field are investigated in Section 3. Section 4 deals with the effects of the local field in a degenerate pump-probe configuration. Finally, Section 5 summarizes the main conclusions.

2 The Bloch equations with local-field corrections

We study the interaction between an external laser field $\mathbf{E} = (1/2)\mathbf{E}_0 e^{-i\omega t} + \text{c.c.}$ with slowly varying amplitude $\mathbf{E}_0$ and angular frequency ω and a medium composed of N spatially distributed V-type atoms. Each atom consists of two upper sublevels $|3\rangle$, $|2\rangle$ coupled to a singlet ground level $|1\rangle$ by one photon transitions. We shall consider the coupling between the V-type atoms and the local field at the atom $\mathbf{E}_L$ which we write as

$$\mathbf{E}_L = \frac{1}{2}\mathbf{E}_{0L} e^{-i\omega t} + \text{c.c.}, \tag{1}$$

$\mathbf{E}_{0L}$ being the slowly varying amplitude of the local field.

In order to take into account the induced-coherence effects by spontaneous emission, the two upper levels $|3\rangle$ and $|2\rangle$ are coupled by the same vacuum modes to the ground level $|1\rangle$. The resonant frequencies between levels $|3\rangle$, $|2\rangle$ and $|1\rangle$ are ω_{31}, and ω_{21}, respectively. Note that $\omega_{31} - \omega_{21} = \omega_{32}$, ω_{32} being the frequency separation of the excited levels. The Hamiltonian of the system in the rotating wave approximation is given by [51]

$$\begin{aligned} H = {} & \hbar \sum_{m=1}^{3} \omega_m \sigma_{mm} + \hbar \sum_{k\lambda} \omega_{k\lambda} a_{k\lambda}^{+} a_{k\lambda} \\ & + \hbar \sum_{m=2}^{3} \sum_{k\lambda} g_{mk} \sigma_{m1} a_{k\lambda} + \text{H.c.} \\ & - \hbar \sum_{m=2}^{3} \left[\Omega_{Lm} e^{-i\omega t} \sigma_{m1} + \text{H.c.} \right], \end{aligned} \tag{2}$$

where H.c. stands for the Hermitian conjugate. Here, $\hbar\omega_m$ are the energies of the atomic levels, $\sigma_{ij} = |i\rangle\langle j|$ are the atomic operators satisfying the usual commutation relations

$$[\sigma_{ij}, \sigma_{pq}] = \sigma_{iq}\delta_{jp} - \sigma_{pj}\delta_{qi}, \tag{3}$$

and the closure property $\sigma_{11} + \sigma_{22} + \sigma_{33} = \mathcal{I}$. $a_{k\lambda}$ ($a_{k\lambda}^{+}$) is the annihilation (creation) operator of the kth mode of the vacuum field with polarization $\mathbf{e}_{k\lambda}$ ($\lambda = 1, 2$) and angular frequency $\omega_{k\lambda}$. The parameter g_{mk} is the coupling constant of the atomic transition $|m\rangle \to |1\rangle$ with the vacuum mode, and is given by

$$g_{mk} = -\sqrt{\frac{\omega_{k\lambda}}{2\hbar\epsilon_0 V}} \left(\boldsymbol{\mu}_{1m} \cdot \mathbf{e}_{k\lambda}\right) \quad m = 2, 3, \tag{4}$$

where $\boldsymbol{\mu}_{1m}$ is the dipolar moment of the transition $|m\rangle \to |1\rangle$, which we assume to be real valued, and V is the mode volume of the field. In addition, the last part of equation (2) represents the interaction of the system with the local electromagnetic field where $\Omega_{Lm} = \boldsymbol{\mu}_{1m} \cdot \mathbf{E}_{0L}/(2\hbar)$ is the Rabi frequency of the transition $|m\rangle \to |1\rangle$ which includes the local field correction. The system is studied using the density-matrix formalism. Following the traditional approach of Weisskopf and Wigner [12,51,52],

we obtain the master equation for the reduced density matrix ρ of the atomic system in an appropriate rotating frame

$$\begin{aligned}\frac{\partial\rho}{\partial t} = &-\frac{\mathrm{i}}{\hbar}\left[H_c,\rho\right] + \frac{1}{2}\gamma_3\left(2\sigma_{13}\rho\sigma_{31} - \sigma_{33}\rho - \rho\sigma_{33}\right)\\ &+ \frac{1}{2}\gamma_2\left(2\sigma_{12}\rho\sigma_{21} - \sigma_{22}\rho - \rho\sigma_{22}\right)\\ &+ \gamma_{32}\left(2\sigma_{12}\rho\sigma_{31} - \sigma_{32}\rho - \rho\sigma_{32}\right)\\ &+ \gamma_{32}\left(2\sigma_{13}\rho\sigma_{21} - \sigma_{23}\rho - \rho\sigma_{23}\right), \end{aligned} \tag{5}$$

where the spontaneous-emission rates from levels $|2\rangle$ and $|3\rangle$ to level $|1\rangle$ are denoted by γ_2 and γ_3, respectively

$$H_c = \hbar\Delta_2\sigma_{22} + \hbar\Delta_3\sigma_{33} - \hbar\sum_{m=2}^{m=3}\left[\Omega_{Lm}\sigma_{m1} + \text{H.c.}\right], \tag{6}$$

is the Hamiltonian of the interaction of the atomic system with the local field $\mathbf{E}_L$ in the frame rotating with the laser frequency ω. We also assume that state $|1\rangle$ is at zero energy. $\Delta_2 = \omega_{21} - \omega$, and $\Delta_3 = \omega_{31} - \omega$, are the detunings of the atomic transitions. Finally, the effect of quantum interference is represented by the terms of the γ_{32} coefficient which is given by [13]

$$\gamma_{32} = \frac{\sqrt{\gamma_3\gamma_2}}{2}\left(\frac{\boldsymbol{\mu}_{13}\cdot\boldsymbol{\mu}_{12}}{\mu_{13}\mu_{12}}\right). \tag{7}$$

The following normalized variables are defined:

$$F_{31} = \frac{2}{\sqrt{\gamma_3\gamma_2}}\left(\frac{\gamma_3}{2} + \mathrm{i}\Delta_3\right), \tag{8}$$

$$F_{21} = \frac{2}{\sqrt{\gamma_3\gamma_2}}\left(\frac{\gamma_2}{2} + \mathrm{i}\Delta_2\right), \tag{9}$$

$$F_{32} = \frac{2}{\sqrt{\gamma_3\gamma_2}}\left[\frac{(\gamma_3+\gamma_2)}{2} + \mathrm{i}(\Delta_3 - \Delta_2)\right], \tag{10}$$

$$x_{Lj} = \frac{2}{\sqrt{\gamma_3\gamma_2}}\Omega_{Lj} \quad (j = 2,3), \tag{11}$$

$$p = \frac{2}{\sqrt{\gamma_3\gamma_2}}\gamma_{32}. \tag{12}$$

By using these definitions, and introducing the normalized time $\tau = \left(\sqrt{\gamma_3\gamma_2}/2\right)t$, the evolution equations of the density matrix elements in the rotating frame take the form [13,14,19]

$$\begin{aligned}\frac{\partial\rho_{33}}{\partial\tau} = &-2\sqrt{\frac{\gamma_3}{\gamma_2}}\rho_{33} - p\left(\rho_{32}+\rho_{23}\right) + \mathrm{i}x_{L3}\rho_{13}\\ &- \mathrm{i}x_{L3}^*\rho_{31}, \end{aligned} \tag{13}$$

$$\begin{aligned}\frac{\partial\rho_{22}}{\partial\tau} = &-2\sqrt{\frac{\gamma_2}{\gamma_3}}\rho_{22} - p\left(\rho_{32}+\rho_{23}\right) + \mathrm{i}x_{L2}\rho_{12}\\ &- \mathrm{i}x_{L2}^*\rho_{21}, \end{aligned} \tag{14}$$

$$\begin{aligned}\frac{\partial\rho_{31}}{\partial\tau} = &-F_{31}\rho_{31} - p\rho_{21} - \mathrm{i}x_{L3}\left(2\rho_{33} + \rho_{22} - 1\right)\\ &- \mathrm{i}x_{L2}\rho_{32}, \end{aligned} \tag{15}$$

$$\begin{aligned}\frac{\partial\rho_{21}}{\partial\tau} = &-F_{21}\rho_{21} - p\rho_{31} + \mathrm{i}x_{L2}\left(1 - \rho_{33} - 2\rho_{22}\right)\\ &- \mathrm{i}x_{L3}\rho_{23}, \end{aligned} \tag{16}$$

$$\begin{aligned}\frac{\partial\rho_{32}}{\partial\tau} = &-F_{32}\rho_{32} - p\left(\rho_{33}+\rho_{22}\right) + \mathrm{i}x_{L3}\rho_{12}\\ &- \mathrm{i}x_{L2}^*\rho_{31}, \end{aligned} \tag{17}$$

where $*$ denotes complex conjugate. This system has been extensively studied to analyze the effect of quantum interference between the two decay channels to the ground level in the absence of LFC. The strength of quantum interference is measured by $p = \boldsymbol{\mu}_{13}\cdot\boldsymbol{\mu}_{12}/(\mu_{13}\mu_{12})$, which denotes the alignment of the two transition moments. Quantum interference is maximum if the transition moment $\boldsymbol{\mu}_{13}$ is parallel to $\boldsymbol{\mu}_{12}$, but it disappears if they are perpendicular.

In our case, we are going to analyze the behavior of the system when the local field correction is taken into account. According to the Lorentz-Lorenz relation [25], the local field is given by

$$\mathbf{E}_L = \mathbf{E} + \frac{\mathbf{P}}{3\epsilon_0}, \tag{18}$$

$\mathbf{P}$ being the macroscopic polarization of the medium. We write the polarization $\mathbf{P}$ as $\mathbf{P} = (1/2)\mathbf{P}_0\mathrm{e}^{-\mathrm{i}\omega t} + \text{c.c.}$, where $\mathbf{P}_0$ is the slowly varying amplitude. In terms of the atomic variables, it can be written as

$$\mathbf{P}_0 = 2N\left(\boldsymbol{\mu}_{13}\rho_{31} + \boldsymbol{\mu}_{12}\rho_{21}\right). \tag{19}$$

Inserting equation (19) in equation (18), we obtain the normalized local field x_{L3} and x_{L2} (Eq. (11)) as

$$x_{L2} = x_2 + \beta\rho_{31} + \alpha_2\rho_{21}, \tag{20}$$

$$x_{L3} = x_3 + \alpha_3\rho_{31} + \beta\rho_{21}, \tag{21}$$

where α_3, α_2 and β are the local field parameters defined as

$$\alpha_3 = \frac{N}{3\hbar\epsilon_0}\frac{2}{\sqrt{\gamma_3\gamma_2}}\mu_{13}^2, \tag{22}$$

$$\alpha_2 = \frac{N}{3\hbar\epsilon_0}\frac{2}{\sqrt{\gamma_3\gamma_2}}\mu_{12}^2, \tag{23}$$

$$\beta = \frac{N}{3\hbar\epsilon_0}\frac{2}{\sqrt{\gamma_3\gamma_2}}\left(\boldsymbol{\mu}_{13}\cdot\boldsymbol{\mu}_{12}\right) = \sqrt{\alpha_3\alpha_2}\,p, \tag{24}$$

and x_j is the normalized external field $x_j = (2/\sqrt{\gamma_3\gamma_2})\Omega_j$, where $\Omega_j = \boldsymbol{\mu}_{1j}\cdot\mathbf{E}_0/(2\hbar)$ is the Rabi frequency of the transition $|j\rangle \to |1\rangle$. By using the modified fields (20, 21) in the density-matrix equations (13–17), we obtain the

following set of nonlinear equations

$$\frac{\partial \rho_{33}}{\partial \tau} = -2\sqrt{\frac{\gamma_3}{\gamma_2}}\rho_{33} - p\left(\rho_{32}+\rho_{23}\right) + \mathrm{i}x_3\rho_{13} - \mathrm{i}x_3^*\rho_{31} + \mathrm{i}\beta\left(\rho_{21}\rho_{13} - \rho_{12}\rho_{31}\right), \quad (25)$$

$$\frac{\partial \rho_{22}}{\partial \tau} = -2\sqrt{\frac{\gamma_2}{\gamma_3}}\rho_{22} - p\left(\rho_{32}+\rho_{23}\right) + \mathrm{i}x_2\rho_{12} - \mathrm{i}x_2^*\rho_{21} + \mathrm{i}\beta\left(\rho_{12}\rho_{31} - \rho_{21}\rho_{13}\right), \quad (26)$$

$$\frac{\partial \rho_{31}}{\partial \tau} = -\left[F_{31} + \mathrm{i}\alpha_3\left(\rho_{33}-\rho_{11}\right) + \mathrm{i}\beta\rho_{32}\right]\rho_{31} - p\left[1 + \mathrm{i}\sqrt{\alpha_2\alpha_3}\left(\rho_{33}-\rho_{11}\right)\right]\rho_{21} - \mathrm{i}x_3\left(\rho_{33}-\rho_{11}\right) - \mathrm{i}\left(x_2+\alpha_2\rho_{21}\right)\rho_{32}, \quad (27)$$

$$\frac{\partial \rho_{21}}{\partial \tau} = -\left[F_{21} + \mathrm{i}\alpha_2\left(\rho_{22}-\rho_{11}\right) + \mathrm{i}\beta\rho_{23}\right]\rho_{21} - p\left[1 + \mathrm{i}\sqrt{\alpha_2\alpha_3}\left(\rho_{22}-\rho_{11}\right)\right]\rho_{31} - \mathrm{i}x_2\left(\rho_{22}-\rho_{11}\right) - \mathrm{i}\left(x_3+\alpha_3\rho_{31}\right)\rho_{23}, \quad (28)$$

$$\frac{\partial \rho_{32}}{\partial \tau} = -F_{32}\rho_{32} - p\left(\rho_{33}+\rho_{22}\right) + \mathrm{i}x_3\rho_{12} - \mathrm{i}x_2^*\rho_{31} + \mathrm{i}\left(\alpha_3-\alpha_2\right)\rho_{31}\rho_{12} + \mathrm{i}\beta\left(|\rho_{21}|^2 - |\rho_{31}|^2\right). \quad (29)$$

There are some interesting differences between equations (25–29) obtained when considering local field effects and those valid for a dilute medium (Eqs. (13–17) without LFC, *i.e.*, $x_{Lj} = x_j$). Let us consider the equation of the temporal evolution of optical coherence ρ_{21} given by equation (28). In this case, the term proportional to ρ_{21} incorporates two additional contributions: the first one arises from the factor $\mathrm{i}\alpha_2(\rho_{22}-\rho_{11})$, and it represents the well-known dynamical detuning. It appears in the local field theory in two-level atoms and leads to the intrinsic optical bistability (IOB) [32,53]. The second one, $\mathrm{i}\beta\rho_{23}$, is a new contribution arising from the combination of quantum interference and the local field. This last term vanishes when the transition dipole moments are orthogonal ($p = 0$). The term in equation (28) proportional to ρ_{31}, which is the naive interference term in dilute V-type system, is also modified by the local field, and it becomes proportional to population inversion. The third term in equation (28) is identical to that in a dilute medium. Finally, the last term in equation (28) is also modified by the local field with regard to equation (16) by a factor $\alpha_3\rho_{31}$, thus representing an effective field coupling of the coherence between the two upper levels. A similar analysis holds for the temporal evolution of ρ_{31} (see Eq. (27)).

Moreover, the population equations, which are not modified by the LFC in two-level atoms and Λ-type atoms, here present an additional term of the type $\mathrm{i}\beta\left(\rho_{21}\rho_{13} - \rho_{12}\rho_{31}\right)$. This new term in the population equations is related to the polarizations of the excited and ground levels. And finally, the temporal evolution of the optical coherence ρ_{32}, given by equation (29), incorporates the local field in two ways: the first contribution is given by $\mathrm{i}(\alpha_3-\alpha_2)\rho_{31}\rho_{12}$, and vanishes when $\gamma_2 = \gamma_3$. The second one is proportional to $\mathrm{i}\beta\left(|\rho_{21}|^2 - |\rho_{31}|^2\right)$, and it represents a combined effect of quantum interference and the local field.

We must pointed out that we have not considered the quantum corrections in our model [37–47]. It is well-known that in the large density regime, radiation trapping of spontaneously emitted photons takes place which limit the validity of our model. In the first field configuration studied (Sect. 3), *i.e.*, a single laser field coupling simultaneously the ground state with the two closely excited states, we have considered the linear regime of the field since in this case the radiation trapping phenomenon is neglected. In the second field configuration analyzed (Sect. 4), we have studied the optical response of the system to a weak probe field coupling one of the optical transition when a strong driving field is coupling the other one. In this last case, the relevance of quantum corrections can not be predicted. For that reason, and in order to check the validity of our model, we have carried out numerical simulations with a model which takes into account the radiation trapping. As a first approximation, we considered our V-type system interaction with a radiation thermal reservoir at finite temperature with a constant mean photon number which means an incoherent pumping mechanism (following the work by Matsko *et al.* [47]). Using this simple model we obtained that the physical behavior does not change significantly. This means that our model (25–29) gives a good qualitative description of the response without considering radiation trapping. Nevertheless, a more detailed study have to be performed to understand the interplay between quantum interference and radiation trapping. This goes beyond the scope of this work, and should be the aim of a future work by the authors.

3 Local field effect with a single driving laser field

In this section we study the influence of the local field when the atom interacts with a single driving field which couples simultaneously the ground state with the two excited levels. The energy-level scheme is shown in Figure 1. In the following, we shall analyze the dynamics as a function of the dimensionless variable $\delta_k \equiv (\Delta_3 + \Delta_2)/\sqrt{\gamma_3\gamma_2}$, which represents the laser detuning from the resonance with the center of the excited levels (see Fig. 1). In order to study the effects of LFC on the response of the system, we have solved equations (25–29). We have chosen the following set of initial conditions: $\rho_{11}(0) = 1$, $\rho_{22}(0) = \rho_{33}(0) = 0$, and $\rho_{ij}(0) = 0$ $(i \neq j)$. After the initial transient, the system reaches the steady state. The final values of coherences and populations obtained for different values of δ_k will be used to analyze the atom-field interaction. We specifically present the absorption characteristics of the optical coherence on the transitions $|1\rangle \rightarrow |3\rangle$ and $|1\rangle \rightarrow |2\rangle$, *i.e.*, $\mathrm{Im}(\rho_{31} + \rho_{21})$, and the behavior of the total population of the two excited sublevels, $(\rho_{33} + \rho_{22})$, as a function of δ_k, for cases with and without LFC. In the rest of the section we shall consider the case $\gamma_3 = \gamma_2 = \gamma$, and $\mu_{13} = \mu_{12} = \mu$, so $x_3 = x_2 \equiv x$, and the local field parameters $\alpha_3 = \alpha_2 \equiv \alpha$, thus $\beta = \alpha p$. We also consider a small frequency separation of the excited levels, $2\omega_{32}/\gamma = 0.03$.

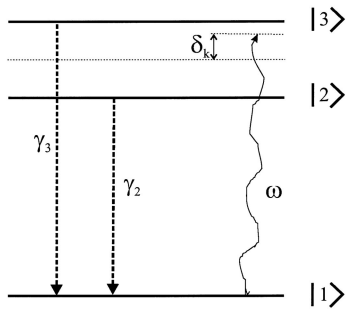

Fig. 1. A V-type atom driven by a single-mode laser with angular frequency ω. γ_3 and γ_2 are the decay rates from the excited sublevels to the ground level. δ_k is the detuning of the coherent field with the central frequency (from the middle point of the two upper levels to level $|1\rangle$).

In order to study the linear response of the atomic system we have calculated the absorption and population in the steady-state regime by using a very low driving field $x = 0.01 \ll 1$. First of all, let us consider the case without quantum interference, *i.e.*, $p = 0$. In this case the dipolar transition moments are orthogonal and we select the external field **E** to be aligned at 45 degrees with regard to both transition moments. The typical behavior of $\mathrm{Im}(\rho_{31}+\rho_{21})$ is depicted in Figure 2a for different values of the local field parameter α. In the absence of LFC, the absorption displays the usual symmetric Lorentzian line shape, where the maximum is placed at zero detuning. However, when LFC is taken into account, the curve shifts to positive detuning values although the shape remains constant. The shift is approximately proportional to the local field parameter (maximum position $\simeq \alpha$). This behavior is due to the additional dynamical detuning included in the coherence (Eqs. (27, 28)), which shifts the resonance condition of the atomic system. This result is quite expected and well-known in two-level systems [53–55].

In the case with maximal quantum interference ($p = 1$), we plot in Figure 2b the linear absorption $\mathrm{Im}(\rho_{31}+\rho_{21})$ as a function of the detuning δ_k for different local field parameters α and a low driving field ($x = 0.01$). In the absence of LFC the usual symmetric curve appears and presents a sharp dip around $\delta_k = 0$. It is well-known that this non-absorption resonance is due to cancellation of the spontaneous emission produced by quantum interference in the two possible decay channels to the ground sublevel. We see in this figure that LFC deforms the absorption curves and breaks the symmetry in δ_k. Note that a sharp dip still remains at zero detuning ($\delta_k = 0$), which means that LFC does not change the non-absorption resonance. Furthermore, at high values of the local field parameter the absorption curve shows a dispersion-like behavior. Finally, it should be noted that for positive values of δ_k the absorption is smaller than for negative values of δ_k in this linear regime of input field.

An interpretation of the peculiarities concerning the influence of local field on the optical behavior of the atomic system can be obtained by looking at the linear stage of the interaction process. In the linear response

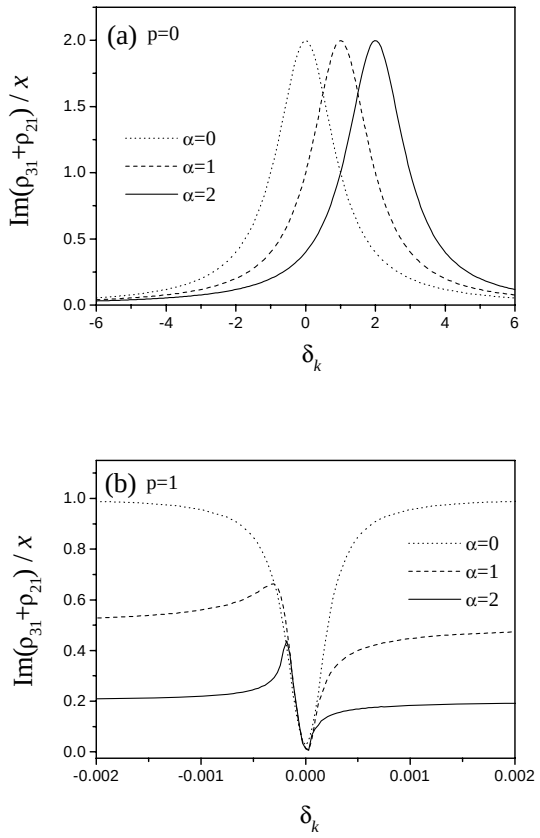

Fig. 2. Imaginary part of the susceptibility $\rho_{31}+\rho_{21}$ *versus* the detuning δ_k for a local field parameter $\alpha = 0$ (dotted curve), $\alpha = 1$ (dashed curve) and $\alpha = 2$ (solid curve). Other parameters are the frequency separation between upper levels $2\omega_{32}/\gamma = 0.03$ and a low driving field $x = 0.01$. The two figures correspond to (a) $p = 0$ and (b) $p = 1$.

regime, where the laser-atom interaction is weak, equations (25–29) may be linearized by assuming that for weak laser fields ρ_{11} remains essentially constant and nearly equal to unity, thus $\rho_{22} \approx \rho_{33} \approx 0$, while the only evolving quantities are coherences ρ_{21} and ρ_{31}. Thus, keeping terms to first order in the field x, equations (27, 28) reduce to

$$\frac{\partial \rho_{31}}{\partial \tau} \simeq -\left(F_{31} - \mathrm{i}\alpha\right)\rho_{31} - p(1-\mathrm{i}\alpha)\rho_{21} + \mathrm{i}x, \qquad (30)$$

$$\frac{\partial \rho_{21}}{\partial \tau} \simeq -\left(F_{21} - \mathrm{i}\alpha\right)\rho_{21} - p(1-\mathrm{i}\alpha)\rho_{31} + \mathrm{i}x. \qquad (31)$$

The steady-state solution of equations (30, 31) is easily obtained, thus the linear absorption is given by

$$\frac{\mathrm{Im}(\rho_{31}+\rho_{21})}{x} = \mathrm{Im}\left\{\frac{2\left[(p-1)(\mathrm{i}+\alpha)+\delta_k\right]}{\left[\delta_k-(p+1)(\mathrm{i}+\alpha)\right]\left[\delta_k+(p-1)(\mathrm{i}+\alpha)\right]-\left(\omega_{32}/\gamma\right)^2}\right\}. \qquad (32)$$

In the case without quantum interference ($p = 0$), equation (32) reduces to

$$\frac{\mathrm{Im}(\rho_{31}+\rho_{21})}{x} = 2\frac{1+(\omega_{32}/\gamma)^2+(\delta_k-\alpha)^2}{4(\delta_k-\alpha)^2+\left[(\delta_k-\alpha)^2\,1-(\omega_{32}/\gamma)^2\right]^2}. \quad (33)$$

This analytical expression agrees with the curves plotted in Figure 2a. The absorption curve presents a nearly Lorentzian shape and the maximum of the absorption curve is approximately placed at $\delta_k = \alpha$. This fact means that the dynamical detuning, added by LFC, shifts the resonance condition to a different detuning value. Note also that in this case the linear evolution of optical coherences ρ_{31} and ρ_{21} become decoupled (see Eqs. (30, 31)). In the case with maximal quantum interference ($p = 1$) the linear absorption curve can be written as

$$\frac{\mathrm{Im}(\rho_{31}+\rho_{21})}{x} = \frac{4\delta_k^2}{4\delta_k^2+\left[-\delta_k^2+(\omega_{32}/\gamma)^2+2\alpha\delta_k\right]^2}. \quad (34)$$

The analytical curves given by equation (34) agree with the curves calculated through the simulations (see Fig. 2b). This curve presents a sharp dip at zero detuning for both cases, with and without LFC, and two maximum at both sides of the resonance condition ($\delta_k = 0$). In the absence of LFC, the two maximum are placed at $\pm\omega_{32}/\gamma$, which leads to a symmetric curve in δ_k. However, when local field is considered, the linear absorption curves become asymmetric (see Fig. 2b). One of the maxima shifts to near zero detuning, $\delta_k \simeq -0.5(\omega_{32}/\gamma)^2/\alpha$, and displays a sharp shape. The other one broadens and shifts to a higher detuning $\delta_k = \alpha + 0.5(\omega_{32}/\gamma)^2/\alpha$. This last absorption maximum behaves roughly as in the case without quantum interference, that is, it follows the shift of the resonance condition due to the additional detuning induced by LFC ($\delta_k \simeq \alpha$).

In summary, we have found that the LFC does not destroy the trapping in the steady-state. A further physical insight on the underlying mechanisms can be obtained by studying the temporal evolution of the absorption and population of the atomic system. Figure 3 shows the time evolution of absorption ($\mathrm{Im}(\rho_{31}+\rho_{21})$) and population ($\rho_{33}+\rho_{22}$) as a function of the normalized time τ for several values of α in the case with $\delta_k = 0$ and $p = 1$. In the absence of LFC ($\alpha = 0$), the system evolves to the trapping state monotonically (dotted line in Fig. 3a). When α increases, both the absorption and population exhibit an oscillatory behavior until reaching the steady-state. It is worth noting that during this time interval the system presents gain with population inversion during part of the cycle, before reaching the final value $\mathrm{Im}(\rho_{31}+\rho_{21}) = 0$. In other words, the effect of LFC is to introduce a temporal retardation in achieving the trapping condition. The origin of this delay arises from the dynamical detuning introduced by the LFC, thus establishing a competition between the quantum interference and the local field. Let us analyze for example the case with $\alpha = 4$ in Figure 3. For low values of τ the partial inversions $\rho_{ii}-\rho_{11}$ ($i = 2, 3$) take negative values, thus establishing an initial detuning in equations (27, 28). As time increases, the excited levels are populated by the action of the external field, so the dynamical detunings are reduced. At the same time, a non zero coherence between upper levels is established, which introduces an additional detuning, and the interference between the two decay paths is being developed. Note that at a certain time, $\mathrm{Im}(\rho_{31}+\rho_{21})$ takes a null value but the system still evolves slightly until reaching the final state. Note also that the time necessary to reach a constant value depends on α. Now we resort again to the linear equations (30, 31) in order to get an explanation of this behavior. In this case we are interested in the transient regime and we look for the homogeneous solution of equations (30, 31). By taking $\delta_k = 0$, and $p = 1$, the complex roots of the corresponding eigenvalue problem are given by

$$\lambda_\pm = -(1-\mathrm{i}\alpha) \pm \sqrt{-(\mathrm{i}+\alpha)^2-(\omega_{32}/\gamma)^2}. \quad (35)$$

The λ_- root is highly damped, so it does not produce observable effects, whereas the λ_+ root is responsible of the

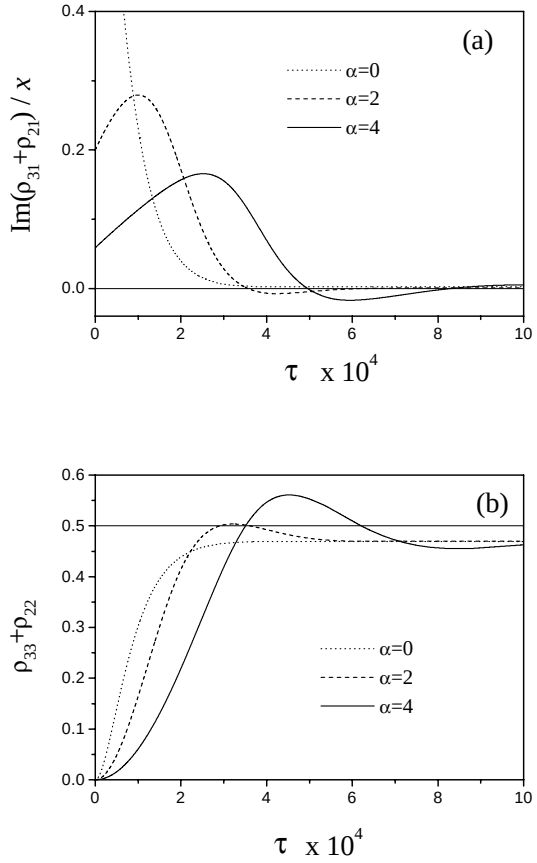

Fig. 3. Temporal evolution of the (a) imaginary part of the susceptibility $\rho_{31}+\rho_{21}$ and (b) population of the excited levels $\rho_{33}+\rho_{22}$ for a local field parameter $\alpha = 0$ (dotted curve), $\alpha = 2$ (dashed curve) and $\alpha = 4$ (solid curve). The rest of parameters are $p = 1$, $\delta_k = 0$, $2\omega_{32}/\gamma = 0.03$ and $x = 0.01$.

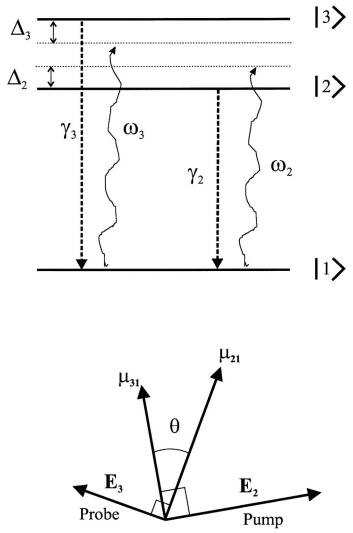

Fig. 4. A V-type configuration. γ_3 and γ_2 are the decay rates from the excited sublevels to the ground level. The ground level is coupled to the excited state $|2\rangle$ with a strong laser field (driving laser $\mathbf{E}_2$) of frequency ω_2. On the other hand, the ground level is coupled to the excited state $|3\rangle$ with a weaker laser field (probe laser $\mathbf{E}_3$) of frequency $\omega_3 = \omega_2$. At the bottom, the polarization arrangement is shown.

oscillations and damping of atomic magnitudes, as shown in Figure 3. We analyzed the dependence of λ_+ on α, and we obtained that both the real and imaginary parts of λ_+ are in the order of 10^{-4} when $\alpha \in [0, 4]$. This result is in accordance with the time scale used in Figure 3. The real part of λ_+ tends to zero as α increases, which explains the time necessary to reach the steady state as indicated in Figure 3. On the other hand, the imaginary part of λ_+ is null for $\alpha = 0$, clearly indicating that oscillations arise from the dynamical detuning, and it is also α-dependent.

4 Local field effects with a drive and probe laser fields

In almost every work done on electromagnetically induced transparency (EIT) and lasing without inversion (LWI), an ensemble of atoms is generally involved with a configuration of a strong driving field which induces the coherence that can lead to gain for a weak probe [19,56]. In three-level atoms, gain may be obtained at wavelengths significantly different from the wavelength of the strong field used. Zhu *et al.* have studied the quenching of spontaneous emission using an open V-type atom, and provided experimental verification of their predictions [22]. Besides, it has been pointed out that the relative phase between the two coherent fields can influence considerably the fluorescence spectrum and the gain of the probe field. Paspalakis *et al.* have used the relative phase to control the spontaneous emission in a four-level system [19]. The same authors have shown that lasing with or without inversion and enhancement of the index of refraction can be obtained in V atoms with closely excited levels, and they showed that these properties are phase dependent [19,20,57]. In this section we analyze the influence of local field in a degenerate pump-probe configuration when the relative phase is accounted for.

We consider the pump-probe configuration shown in Figure 4. The transition dipole moments $\boldsymbol{\mu}_{13}$ and $\boldsymbol{\mu}_{12}$ are non orthogonal. The pump field ($\mathbf{E}_{02}\mathrm{e}^{-\mathrm{i}\phi_2}$) drives the $|2\rangle \rightarrow |1\rangle$ transition ($\boldsymbol{\mu}_{13} \cdot \mathbf{E}_{02} = 0$) and similarly the probe field ($\mathbf{E}_{03}\mathrm{e}^{-\mathrm{i}\phi_3}$) drives the $|3\rangle \rightarrow |1\rangle$ transition ($\boldsymbol{\mu}_{12} \cdot \mathbf{E}_{03} = 0$). The energy-level scheme is shown in Figure 4 together with the arrangement of the field polarizations [56]. We assume both fields with equal angular frequency. Therefore, the total field is given by

$$\mathbf{E}_0 = \mathbf{E}_{02}\mathrm{e}^{-\mathrm{i}\phi_2} + \mathbf{E}_{03}\mathrm{e}^{-\mathrm{i}\phi_3}. \tag{36}$$

By taking into account the above polarization restrictions, we arrive at the following relations between the normalized fields and the quantum interference parameter $p = \boldsymbol{\mu}_{13} \cdot \boldsymbol{\mu}_{12}/(\mu_{13}\mu_{12}) = \cos(\theta)$:

$$\begin{aligned} x_3 &= \frac{2}{\sqrt{\gamma_3\gamma_2}}\frac{\mu_{13}E_{03}\sin(\theta)}{2\hbar}\mathrm{e}^{-\mathrm{i}\phi_3} = |x_3|\mathrm{e}^{-\mathrm{i}\phi_3} \\ &= x_3^0\sqrt{1-p^2}\mathrm{e}^{-\mathrm{i}\phi_3}, \end{aligned} \tag{37}$$

$$\begin{aligned} x_2 &= \frac{2}{\sqrt{\gamma_3\gamma_2}}\frac{\mu_{12}E_{02}\sin(\theta)}{2\hbar}\mathrm{e}^{-\mathrm{i}\phi_2} = |x_2|\mathrm{e}^{-\mathrm{i}\phi_2} \\ &= x_2^0\sqrt{1-p^2}\mathrm{e}^{-\mathrm{i}\phi_2}. \end{aligned} \tag{38}$$

By using these normalized fields (37, 38) in density-matrix equations (25–29), we transform to a new frame with

$$\rho_{31} = \rho_{31}\mathrm{e}^{-\mathrm{i}\phi_3}, \tag{39}$$

$$\rho_{21} = \rho_{21}\mathrm{e}^{-\mathrm{i}\phi_2}, \tag{40}$$

$$\rho_{32} = \rho_{32}\mathrm{e}^{-\mathrm{i}(\phi_3-\phi_2)} = \rho_{32}\mathrm{e}^{-\mathrm{i}\phi}, \tag{41}$$

thus obtaining the following set of nonlinear equations (for the sake of simplicity we use the same notation for the ρ_{ij} elements in both frames)

$$\begin{aligned} \frac{\partial\rho_{33}}{\partial\tau} &= -2\sqrt{\frac{\gamma_3}{\gamma_2}}\rho_{33} - p\left(\rho_{32}\mathrm{e}^{-\mathrm{i}\phi} + \rho_{23}\mathrm{e}^{\mathrm{i}\phi}\right) \\ &\quad + \mathrm{i}|x_3|\left(\rho_{13} - \rho_{31}\right) + \mathrm{i}\beta\left(\rho_{21}\rho_{13}\mathrm{e}^{\mathrm{i}\phi} - \rho_{12}\rho_{31}\mathrm{e}^{-\mathrm{i}\phi}\right), \end{aligned} \tag{42}$$

$$\begin{aligned} \frac{\partial\rho_{22}}{\partial\tau} &= -2\sqrt{\frac{\gamma_2}{\gamma_3}}\rho_{22} - p\left(\rho_{32}\mathrm{e}^{-\mathrm{i}\phi} + \rho_{23}\mathrm{e}^{\mathrm{i}\phi}\right) \\ &\quad + \mathrm{i}|x_2|\left(\rho_{12} - \rho_{21}\right) + \mathrm{i}\beta\left(\rho_{31}\rho_{12}\mathrm{e}^{-\mathrm{i}\phi} - \rho_{13}\rho_{21}\mathrm{e}^{\mathrm{i}\phi}\right), \end{aligned} \tag{43}$$

$$\begin{aligned} \frac{\partial\rho_{31}}{\partial\tau} &= -\left[F_{31} + \mathrm{i}\alpha_3\left(\rho_{33} - \rho_{11}\right) + \mathrm{i}\beta\rho_{32}\mathrm{e}^{-\mathrm{i}\phi}\right]\rho_{31} \\ &\quad - p\rho_{21}\mathrm{e}^{\mathrm{i}\phi} - \mathrm{i}|x_3|\left(\rho_{33} - \rho_{11}\right) \\ &\quad - \mathrm{i}\left(|x_2| + \alpha_2\rho_{21}\right)\rho_{32} - \mathrm{i}\beta\rho_{21}\mathrm{e}^{\mathrm{i}\phi}\left(2\rho_{33} + \rho_{22} - 1\right), \end{aligned} \tag{44}$$

$$\frac{\partial \rho_{21}}{\partial \tau} = -\left[F_{21} + \mathrm{i}\alpha_2\left(\rho_{22}-\rho_{11}\right) + \mathrm{i}\beta\rho_{23}\mathrm{e}^{\mathrm{i}\phi}\right]\rho_{21} - p\rho_{31}\mathrm{e}^{-\mathrm{i}\phi} - \mathrm{i}|x_2|\left(\rho_{22}-\rho_{11}\right) - \mathrm{i}\left(|x_3| + \alpha_3\rho_{31}\right)\rho_{23} + \mathrm{i}\beta\rho_{31}\left(\rho_{11}-\rho_{22}\right)\mathrm{e}^{-\mathrm{i}\phi}, \quad (45)$$

$$\frac{\partial \rho_{32}}{\partial \tau} = -F_{32}\rho_{32} - p\mathrm{e}^{\mathrm{i}\phi}\left(\rho_{33}+\rho_{22}\right) + \mathrm{i}\left(|x_3| + \alpha_3\rho_{31}\right)\rho_{12} - \mathrm{i}\left(|x_2| + \alpha_2\rho_{12}\right)\rho_{31} + \mathrm{i}\beta\left(|\rho_{12}|^2 + |\rho_{13}|^2\right)\mathrm{e}^{\mathrm{i}\phi}. \quad (46)$$

It is worth mentioning that the new terms induced in these equations by the local field parameter β also depend on ϕ. Note this dependence occurs only in the case where $p \neq 0$.

Following, we shall analyze the dynamics as a function of the dimensionless probe laser detuning, $2\Delta_3/\sqrt{\gamma_3\gamma_2}$. We consider the pump field to be on resonance with transition $|2\rangle \rightarrow |1\rangle$, *i.e.*, $\Delta_2 = 0$. This condition implies that $\Delta_3 \simeq \omega_{32}$ (see Fig. 4), so tuning the probe laser means changing the separation between the excited levels. In order to study the effect of LFC on the response of the system, we have solved the equations (42–46) with the following set of initial conditions: $\rho_{11}(0) = 1$, $\rho_{22}(0) = \rho_{33}(0) = 0$ and $\rho_{ij}(0) = 0$ $(i \neq j)$. After an initial transient, the system reaches a steady state. We are interested in the steady state behavior of the probe transition $|3\rangle \rightarrow |1\rangle$, that is, in the population difference $(\rho_{33} - \rho_{11})$, and in the probe absorption of the system which is computed as follows [58]: the polarization ρ_{31} can be approximated by

$$\rho_{31} = \rho_{31}^{(0)} + \rho_{31L}\, x_3, \quad (47)$$

where $\rho_{31}^{(0)} \equiv \rho_{31}(x_3 = 0)$ is the lowest order nonlinear susceptibility (see Eq. (7) in Ref. [58]). Then, the probe absorption is related with the imaginary part of $(\rho_{31} - \rho_{31}^{(0)})/x_3 \equiv \rho_{31L}$. In this way, a negative value of $\mathrm{Im}(\rho_{31L})$ implies that the system exhibits gain.

First, let us consider the effect of LFC on the behavior of the system without quantum interference ($p = 0$) and equal decay rates, $\gamma_3 = \gamma_2$. Figure 5 presents the steady-state of population difference $\rho_{33} - \rho_{11}$ and the absorption $\mathrm{Im}(\rho_{31L})$ *versus* the dimensionless probe laser detuning for the cases with and without LFC. Both magnitudes have a double-peaked shape centered at $\Delta_3 = 0$, and the two absorption peaks are located at $2\Delta_3/\sqrt{\gamma_3\gamma_2} = \pm|x_2|$, corresponding to the transitions between state $|3\rangle$ and the Autler-Townes doublet (dressed states) generated by the strong coherent field $|x_2|$. We can see that the effect of the local field is to shift the peaks to positive detunings. Note that in the case where $p = 0$, transition $|3\rangle \rightarrow |1\rangle$ is weakly coupled to $|2\rangle \rightarrow |1\rangle$ since the terms with p and β vanish in equation (44), and the influence of LFC is represented by the dynamical detuning $(\mathrm{i}\alpha_3(\rho_{33} - \rho_{11}))$, and the second order term $-\mathrm{i}\alpha_2\rho_{21}\rho_{32}$.

As noted in the previous section, the case with quantum interference will offer new possibilities. As we have mentioned above, the strength of quantum interference must be smaller than 1, thus in the following we assume

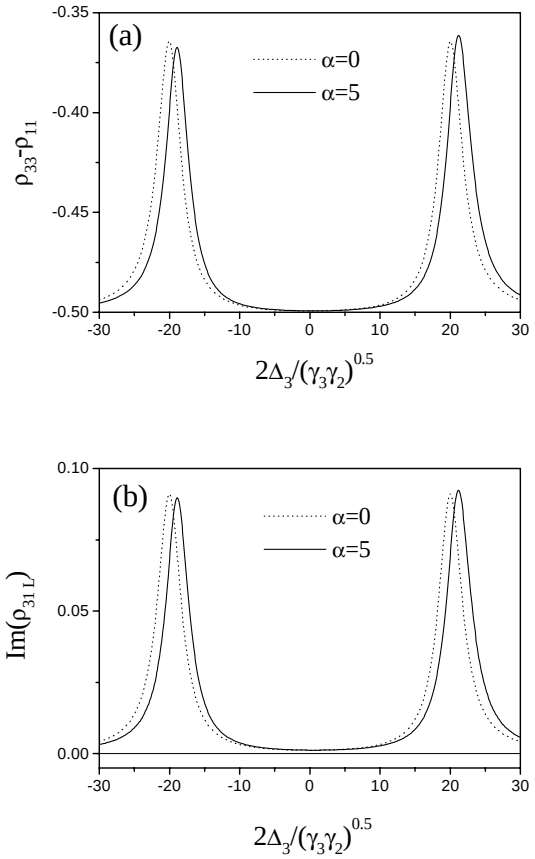

Fig. 5. (a) Population difference $\rho_{33} - \rho_{11}$ and (b) imaginary part of the susceptibility ρ_{31L} *versus* the dimensionless probe detuning $2\Delta_3/\sqrt{\gamma_3\gamma_2}$ for a local field parameter $\alpha = 0$ (dotted curve) and $\alpha = 5$ (solid curve). The rest of parameters are; $p = 0$, $\gamma_3 = \gamma_2$, $x_3^0 = 1$, $x_2^0 = 20$, $\Delta_2 = 0$, and $\phi = 0$.

$p = 0.99$. We will consider both fields to be in phase ($\phi = 0$) and the same decay rates $\gamma_3 = \gamma_2$ for the transitions. In the absence of LFC, inversion is plotted in Figure 6a (dotted curve) and probe absorption is shown in Figure 6b. Both magnitudes show a symmetric double-peaked shape. Note that neither gain (negative value of $\mathrm{Im}(\rho_{31L})$) nor inversion (positive value of $\rho_{33} - \rho_{11}$) appear. The peaks are located at $2\Delta_3/\sqrt{\gamma_2\gamma_3} = \pm x_2^0\sqrt{1-p^2}$, which in modulus represents the effective Rabi frequency. The behavior is very similar to the case where $p = 0$. Nevertheless, significant changes take place when LFC is considered. In relation with population difference $(\rho_{33} - \rho_{11})$, we obtain that both peaks increase and reach positive values, *i.e.*, inversion is allowed at certain detuning intervals. Moreover, one of the two peaks, the ones placed at positive detunings, narrows, while the other peak broadens (see Fig. 6a).

The probe absorption in the case $\alpha = 2$ becomes asymmetric on either side of zero detuning, although the general behavior is very similar to the case $\alpha = 0$. However, when LFC increases to $\alpha = 4$, a dramatic change occurs. The solid curve in Figure 6b shows that the Autler-Townes component at positive detuning presents a dispersive-like shape with a gain region. This gain is accompanied by

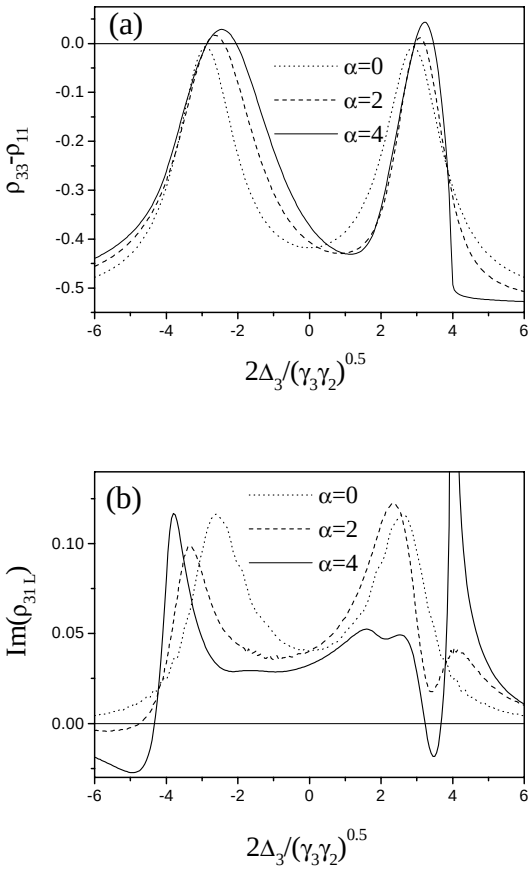

Fig. 6. (a) Population difference $\rho_{33} - \rho_{11}$ and (b) imaginary part of the susceptibility ρ_{31L} *versus* the dimensionless probe detuning $2\Delta_3/\sqrt{\gamma_3\gamma_2}$ for a local field parameter $\alpha = 0$ (dotted curve), $\alpha = 2$ (dashed curve), and $\alpha = 4$ (solid curve). The rest of parameters are; $p = 0.99$, $\gamma_3 = \gamma_2$, $x_3^0 = 1$, $x_2^0 = 20$, $\Delta_2 = 0$, and $\phi = 0$.

positive inversion. Therefore LFC induces gain with inversion. Another remarkable effect induced by the presence of the local field and quantum interference is the strong absorption peak five times stronger at its maximum value than the analogous case without local field ($\alpha = 0$). This peak appears very near to the gain region, so a slightly change in the probe detuning can lead the system from the strong absorption region to the gain region.

In the absence of LFC and with quantum interference, it is well-known that by reducing the decay constant of the probe transition ($\gamma_3 < \gamma_2$), the system exhibits gain with inversion [58]. Figure 7 shows the probe absorption *versus* the dimensionless detuning $2\Delta_3/\sqrt{\gamma_3\gamma_2}$ by using a ratio between the decay constants $\gamma_3/\gamma_2 = 0.5$, with and without LFC. In the absence of LFC we recover the results obtained by Gong *et al.* [58]: two symmetric gain regions placed at the Autler-Townes doublet appear. Whereas if $\alpha_2 \neq 0$, the left-side component of the doublet flips sign and the other is highly enhanced.

In all the previous cases the relative phase ϕ was set to zero. Now, we analyze the optical behavior of the system when the relative phase between the two coherent

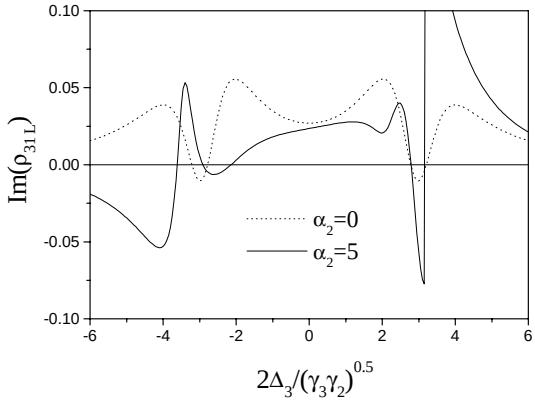

Fig. 7. Imaginary part of the susceptibility ρ_{31L} *versus* the dimensionless probe detuning $2\Delta_3/\sqrt{\gamma_3\gamma_2}$ for a local field parameter $\alpha = 0$ (dotted curve) and $\alpha_2 = 5$ (solid curve). The rest of parameters are; $p = 0.99$, $\gamma_3/\gamma_2 = 0.5$, $x_3^0 = 1$, $x_2^0 = 20$, $\Delta_2 = 0$, and $\phi = 0$.

fields is varied. It is well-known that, in the absence of LFC and with quantum interference, V-type atoms exhibits a phase-dependent population inversion [58]. Thus a phase dependence is expected on the dynamical detuning induced by LFC. Figure 8a shows the probe absorption for $\alpha_2 = 5$, $\gamma_3/\gamma_2 = 0.5$, and two values of the relative phase. In the case where $\phi = \pi/2$, the system presents three regions with gain. The left-side component of the doublet flips sign, while the other is slightly displaced when ϕ changes from 0 to $\pi/2$. In the central region of gain, EIT can still be obtained in contrast with the case where $\alpha_2 = 0$. That is, the combined effect of the relative phase and LFC plays an important role in the gain behavior. To emphasize this point, Figure 8b presents the probe absorption as a function of the relative phase, when the probe is tuned near the left Autler-Townes component ($2\Delta_3/\sqrt{\gamma_3\gamma_2} = -3.45$). By varying the relative phase, the probe laser may experience gain, transparency or absorption.

5 Conclusions

In summary, we have analyzed the influence of near dipole-dipole interaction in a dense collection of V-type atoms when quantum interference between the two decay channels to the ground atomic level is considered. We have analyzed the effects of LFC using a single laser field in the linear regime coupling simultaneously the ground state with the two excited levels. We have illustrated that coherent population trapping is not destroyed when LFC is considered. In particular, we have shown that the non-absorption dip persists. LFC introduces a time delay to attain the effective population trapping. We have shown that this time delay increases as the strength of the LFC increases. This result may be explained qualitatively by considering the linear equations (30, 31) in the transient regime. Our results are in accordance with those reported by Jyotsna and Agarwal [50] in a dense collection of Λ-type

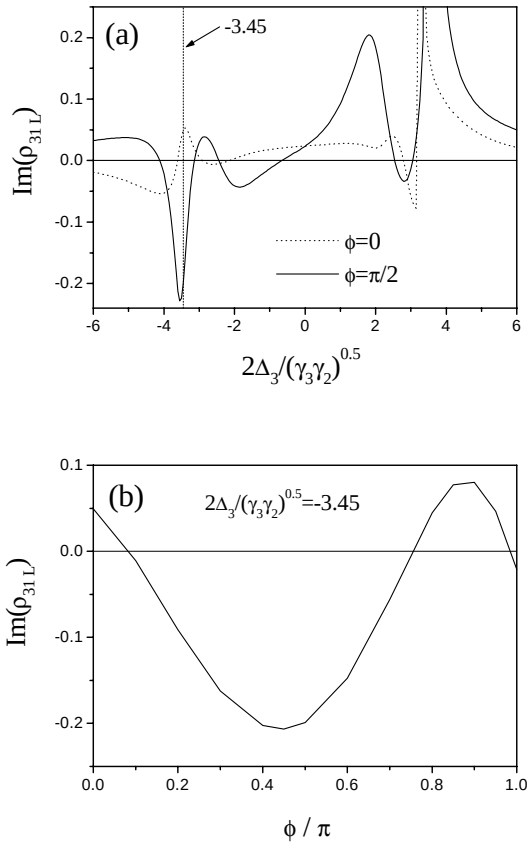

Fig. 8. (a) Imaginary part of the susceptibility ρ_{31L} *versus* the dimensionless probe detuning $2\Delta_3/\sqrt{\gamma_3\gamma_2}$ for a relative phase $\phi = 0$ (dotted curve) and $\phi = \pi/2$ (solid curve). We use a local field parameter $\alpha_2 = 5$. The rest of parameters are; $p = 0.99$, $\gamma_3/\gamma_2 = 0.5$, $x_3^0 = 1$, $x_2^0 = 20$, and $\Delta_2 = 0$. (b) Imaginary part of the susceptibility ρ_{31L} *versus* the relative phase ϕ for a dimensionless probe detuning $2\Delta_3/\sqrt{\gamma_3\gamma_2} = -3.45$. The rest of parameters are the same than in (a).

atoms. In the absence of quantum interference, no trapping is obtained even by considering LFC. The imaginary part of the susceptibility curve remains essentially unaltered in shape and shifts to positive detunings. This is an expected result which is well-known in two-level systems.

We have analyzed the effects of LFC in a degenerate pump-probe configuration. In the absence of quantum interference the most relevant result is concerned with the shift of the Autler-Townes doublet to positive detunings, which can be interpreted as a consequence of the frequency renormalization introduced by the dynamical detuning. In the case with quantum interference, equal decay rates and both fields to be in phase, a change from absorption to gain with inversion in one of the components of the doublet is obtained by raising the magnitude of LFC. At different decay rates of the two upper transitions the gain in one of the components of the doublet is enhanced whereas the other component is strongly distorted exhibiting the possibility of null absorption at certain detuning. Finally the effect of the relative phase between the pump and probe fields, manifests itself through a dramatic change in the probe absorption (see Fig. 8): it is possible to change one of the Autler-Townes component from absorption to gain depending on the value of this relative phase. This last effect appears only if quantum interference and LFC are present simultaneously.

When quantum interference is considered the interpretation of the effects of LFC reveals as a complex task which arises from the nonlinear couplings involved.

We are gratefully to Tomás Lorca for the correction of the manuscript. This work was supported by project No. BFM2000-0796 (Spain).

References

1. S.E. Harris, J.E. Field, A. Imamouglu, Phys. Rev. Lett. **64**, 1107 (1990)
2. K.J. Boller, A. Imamouglu, S.E. Harris, Phys. Rev. Lett. **66**, 2593 (1991)
3. O. Kocharovskaya, Y.I. Khanin, JETP Lett. **48**, 580 (1988)
4. S.E. Harris, Phys. Rev. Lett. **62**, 1033 (1989)
5. M.O. Scully, S.-Y. Zhu, A. Gavrielides, Phys. Rev. Lett. **62**, 2813 (1989)
6. M.O. Scully, M. Fleischhauer, Phys. Rev. Lett. **67**, 1885 (1991)
7. S.E. Harris, J.E. Feld, A. Kasapi, Phys. Rev. A **46**, R29 (1992)
8. M. Fleischhauer, C.H. Keitel, M.O. Scully, Ch. Su, B.T. Ulrich, S.-Y. Zhu, Phys. Rev. A **46**, 1468 (1992)
9. M.O. Scully, M. Fleischhauer, Phys. Rev. Lett. **69**, 1360 (1992)
10. K. Hakuta, L. Marmet, B.P. Stoicheff, Phys. Rev. Lett. **66**, 596 (1991)
11. S.E. Harris, Phys. Rev. Lett. **72**, 52 (1994)
12. G.S. Agarwal, *Quantum Optics*, Springer Tracts in modern Physics (Springer, Berlin, 1974), Vol. 70
13. P. Zhou, S. Swain, Phys. Rev. A **56**, 3011 (1997)
14. G.S. Agarwal, Phys. Rev. A **18**, 1490 (1978)
15. L.M. Narducci, M.O. Scully, G.L. Oppo, P. Ru, J.R. Tredicce, Phys. Rev. A **42**, 1630 (1990)
16. P. Zhou, S. Swain, Phys. Rev. Lett. **77**, 3995 (1996)
17. E. Arimondo, Prog. Opt. **35**, 257 (1996)
18. H. Lee, P. Polynkin, M.O. Scully, S.Y. Zhu, Phys. Rev. A **55**, 4454 (1997)
19. E. Paspalakis, N.J. Kyltra, P.L. Knight, Phys. Rev. Lett. **82**, 2079 (1999); Phys. Rev. A **61**, 045802 (2000)
20. E. Paspalakis, P.L. Knight, Phys. Rev. Lett. **81**, 293 (1998)
21. D.A. Cardimona, M.G. Raymer, C.R. Stroud, J. Phys. B **15**, 55 (1982); J. Phys. Lett. **81**, 293 (1998)
22. S.-Y. Zhu, M.O. Scully, Phys. Rev. Lett. **76**, 388 (1996)
23. H. Schmidt, A. Imamoglu, Opt. Commun. **131**, 333 (1996)
24. G.S. Agarwal, A.K. Patnaik, Phys. Rev. A **63**, 043805 (2001)
25. J.D. Jackson, *Classical electrodynamics* (Wiley, New York, 1962)
26. C.M. Bowden, A. Postan, R. Inguva, J. Opt. Soc. Am. **8**, 1081 (1991)
27. C.R. Stroud, C.M. Bowden, L. Allen, Opt. Commun. **67**, 386 (1988)
28. R. Friedberg, S.R. Hartmann, J.T. Manassah, Phys. Rep. **7**, 101 (1973); **39**, 3444 (1989); **40**, 2446 (1989)

29. J.J. Maki, M.S. Malcuit, J.E. Sipe, R.W. Boyd, Phys. Rev. Lett. **67**, 972 (1991)
30. M.E. Crenshaw, M. Scalora, C.M. Bowden, Phys. Rev. Lett. **68**, 911 (1992)
31. F.A. Hopf, C.M. Bowden, W. Louisell, Phys. Rev. A **29**, 2591 (1984)
32. Y. Ben-Aryeh, C.M. Bowden, J.C. Englund, Phys. Rev. A **34**, 3917 (1986)
33. J.W. Haus, L. Wang, M. Scalora, C.M. Bowden, Phys. Rev. A **38**, 4043 (1988)
34. R. Inguva, C.M. Bowden, Phys. Rev. A **41**, 1670 (1990)
35. M.P. Hehlen, H.U. Güdel, Q. Shu, J. Rai, S. Rai, S.C. Rand, Phys. Rev. Lett. **73**, 1103 (1994)
36. C.M. Bowden, Phys. World **7**, 24 (1994)
37. G. Nienhuis, C.T. Alkemade, Physica C **81**, 181 (1976)
38. J. Knoester, S. Mukamel, Phys. Rev. A **40**, 7065 (1989)
39. R.J. Glauber, M. Lewenstein, Phys. Rev. A **43**, 467 (1991)
40. G.L.J.A. Rikken, Y.A.R.R. Kessener, Phys. Rev. Lett. **74**, 880 (1995)
41. F.J.P. Schuurmans, D.T.N. de Lang, G.H. Wegdam, R. Sprik, A. Lagendijk, Phys. Rev. Lett. **80**, 5077 (1998)
42. P. de Vries, A. Lagendijk, Phys. Rev. Lett. **81**, 1381 (1998)
43. S. Scheel, L. Knoll, D.G. Welsch, S.M. Barnett, Phys. Rev. A **60**, 1590 (1999)
44. M. Fleischhauer, S.F. Yelin, Phys. Rev. A **59**, 2427 (1999)
45. M. Fleischhauer, Phys. Rev. A **60**, 2534 (1999)
46. M.E. Crenshaw, C.M. Bowden, Phys. Rev. Lett. **85**, 1851 (2000)
47. A.B. Matsko, I. Novikova, M.O. Scully, G.R. Welch, Phys. Rev. Lett. **87**, 133601 (2001)
48. J.P. Dowling, C.M. Bowden, Phys. Rev. Lett. **10**, 1421 (1993)
49. A.S. Manka, J.P. Dowling, C.M. Bowden, M. Fleischhauer, Quant. Opt. **6**, 371 (1994)
50. I.V. Jyotsna, G.S. Agarwal, Phys. Rev. A, **53**, 3 (1996)
51. M.O. Scully, M.S. Zubairy, *Quantum Optics* (Cambridge University Press, London, 1997)
52. J.-S. Peng, L. Gao-Xiang, *Introduction to Modern Quantum Optics* (World Scientific, Singapore, 1998), Ch. 14
53. R. Friedberg, S.R. Hartmann, J.T. Manassah, Phys. Rev. A **40**, 2446 (1989)
54. C.M. Bowden, J.P. Dowling, Phys. Rev. A **47**, 1247 (1993)
55. V.A. Sautenkov, H. van Kampen, E.R. Eliel, J.P. Woerdman, Phys. Rev. Lett. **77**, 3327 (1996)
56. S. Menon, G.S. Agarwal, Phys. Rev. A **61**, 013807 (1999)
57. E. Paspalakis, P.L. Knight, J. Mod. Opt. **47**, 1025 (2000)
58. S.-Q. Gong, E. Paspalakis, P.L. Knight, J. Mod. Opt. **45**, 2433 (1998)